Contribution from the Department of Chemistry,
University of Houston, Houston, Texas 77004

Counterion and Solvent Effects on the Electrode Reactions of Iron Porphyrins[1]

L. A. BOTTOMLEY and K. M. KADISH*

Received October 10, 1980

The first, systematic study of the interacting effects of solvent and axially coordinated monovalent anions on the electroreduction mechanisms and redox potentials of iron porphyrins is presented. Five different anions were coordinated to (5,10,15,20-tetraphenylporphinato)iron(III), and their respective redox reactions were investigated in 12 nonaqueous solvents. Potential shifts with changes in solvent were directly related to solvent donicity. Potential shifts with changes in counterion were related to the degree of iron(III)–counterion interaction and were also found to be solvent dependent. The counterion is the predominant factor governing the type of electron-transfer mechanism observed for the electrode reactions of iron porphyrins. With the results obtained, the apparent independence of redox potentials of the iron-center spin state is established.

Introduction

Recent spectroscopic investigations of iron porphyrins have been aimed toward elucidating the dependence of axial ligand and/or counterion coordination on the spin state of the Fe atom. Most electrochemical studies of synthetic iron porphyrins have been carried out in nonaqueous media with the five-coordinate high-spin complexes OEPFeCl[2] and TPPFeCl, usually in DMF, Me_2SO, or CH_2Cl_2.[3,4] It is only recently that the electrochemistry of the intermediate-spin complex $TPPFeClO_4$, as well as other complexes of TPPFeX, has been investigated, but these studies were limited primarily to a single solvent system, CH_2Cl_2.[5-9]

In earlier papers initial data were presented on how half-wave potentials for Fe(III)/Fe(II) reaction of TPPFeCl vary as a function of solvent.[10,11] This paper presents the first systematic investigation of how the counterion associated with $TPPFe^+$ and solvent system influence potentials for metal-centered redox reactions of iron(III) and iron(II) porphyrins. We have greatly expanded on the work in the literature by investigating complexes of TPPFeX with five different counterions in 12 different solvents. Special emphasis has been placed on the electrode reactions in Me_2SO, DMF, and CH_2Cl_2. The reactions in neat pyridine have been discussed in a previous publication.[7] On the basis of these studies a clear picture of the interdependence of solvent–counterion coordination to the Fe(III) center emerges. Finally, the independence of the spin state from the iron(III) and iron(II) porphyrin reduction potential will be demonstrated.

Experimental Section

Methods. Polarographic measurements were made with use of an EG&G Princeton Applied Research (PAR) Model 174A polarographic analyzer utilizing the three-electrode configuration with a dropping-mercury electrode (DME), a platinum-wire counterelectrode, and commercial saturated calomel reference electrode (SCE). An Omnigraphic 2000 X-Y recorder was used to record the current–voltage output. Cyclic voltammetric measurements were made by using one of two different experimental setups. For measurements made in the slow scan rate domain the PAR Model 174A was used with a Houston Omnigraphic 2000 X-Y recorder to display the current–voltage curves obtained. A three-electrode configuration was employed with a Pt-button working electrode, a Pt-wire counterelectrode, and a commercially obtained SCE as the reference electrode. Measurements in the fast scan rate domain were made with a PAR Model 173 potentiostat/galvanostat and Model 178 electrometer probe driven by either a PAR 175 universal programmer or a Hewlett-Packard Model 3310B function generator. Current–voltage curves were taken at sweep rates between 0.50 and 50.0 V/s and were collected on a Tektronix Model 5111 storage oscilloscope with camera attachment. A three-electrode system was employed similar to that described above. IR loss was held to a minimum by use of a positive feedback device built into the Model 179 digital coulometer or Model 176 current follower plug-ins for the potentiostat. Sweep rates were varied between 0.02 and 50.0 V/s.

For all electrochemical experiments, the reference electrode was separated from the solution by means of a fritted bridge filled with solvent and supporting electrolyte. The solution in the bridge was changed periodically to prevent aqueous contamination of the cell solution by the reference electrode. Deaeration of all solutions was accomplished by passing a constant stream of high-purity nitrogen through the solution for 10 min and maintaining a blanket of nitrogen over the solution while the measurements were made. The nitrogen was saturated with solvent prior to entering the cell. Half-wave potentials were measured as the average of the anodic and cathodic peak potentials $(E_{p,a} + E_{p,c})/2$. All potentials are reported vs. the SCE and have a maximum associated uncertainty of ±0.01 V.

A Model 31 YSI conductivity bridge was used to measure solution conductances. Measurements were taken in a Metrohm AG Herisaur Model EA 655 cell (cell constant = 0.092 cm^{-1}) which was immersed in a constant-temperature bath of 25.00 ± 0.05 °C. All values are reported as molar conductances.

Visible spectroscopic measurements were made with a Tracor Northern 1710 holographic optical spectrometer/multichannel analyzer. Spectra result from the signal averaging of 100 sequential 5-ms spectral acquisitions. Each acquisition represents a single spectrum from 350 to 750 nm simultaneously recorded by a silicon diode array detector with a resolution of 1.2 nm per channel.

Materials. The supporting electrolytes TBABr, TBACl, TBAP, and TBAF were obtained from Eastman Chemicals and were dried in vacuo prior to use. TBAP was first recrystallized from ethyl acetate and then dried in vacuo at 80 °C. $TBABF_4$ and $TBAPF_6$ were used as received from Fluka.

TPPFeCl and $(TPPFe)_2O$ were used as received from Strem Chemical Co. or were synthesized as per the method of Adler et al.[12]

(1) Abstracted in part from the Ph.D. dissertation of L. A. Bottomley, University of Houston, 1980, and presented in part at the 179th National Meeting of the American Chemical Society, Houston, Texas, March 1980; see Abstracts, No. INOR 148.
(2) Abbreviations: TPP^{2-}, 5,10,15,20-tetraphenylporphinato dianion; OEP^{2-}, octaethylporphinato dianion; DN, Gutmann donor number; X, monovalent anion; L, ligand molecule; S, solvent molecule; β_n^m, formation constant for the addition of n molecules to metalloporphyrin complex with the metal in the m oxidation state; py, pyridine; $EtCl_2$, 1,2-dichloroethane; PrCN, *n*-butyronitrile; PhCN, benzonitrile; THF, tetrahydrofuran; Me_2SO, dimethyl sulfoxide; DMF, *N,N*-dimethylformamide; DMA, *N,N*-dimethylacetamide; TBAP, tetrabutylammonium perchlorate; $TBAPF_6$, tetrabutylammonium hexafluorophosphate; $TBABF_4$, tetrabutylammonium tetrafluoroborate; TBABr, tetrabutylammonium bromide; TBACl, tetrabutylammonium chloride; TBAF, tetrabutylammonium fluoride.
(3) R. H. Felton in "The Porphyrins", Vol. V, D. Dolphin, Ed., Academic Press, New York, 1978, Chapter 3.
(4) D. G. Davis in "The Porphyrins", Vol. V, D. Dolphin, Ed., Academic Press, New York, 1978, Chapter 4.
(5) K. M. Kadish and L. A. Bottomley, *Inorg. Chem.*, **19**, 832 (1980).
(6) I. A. Cohen, D. K. Lavallee, and A. B. Kopeloue, *Inorg. Chem.*, **19**, 1098 (1980).
(7) L. A. Bottomley, R. K. Rhodes, and K. M. Kadish, Proceedings of the Symposium on Interaction Between Iron and Proteins in Oxygen and Electron Transport, 1980.
(8) M. Phillippi and H. Goff, *Inorg. Chem.*, in press.
(9) K. M. Kadish, L. A. Bottomley, J. Brace, and N. Winograd, *J. Am. Chem. Soc.*, **102**, 4341 (1980).
(10) K. M. Kadish, M. M. Morrison, L. A. Constant, L. Dickens, and D. G. Davis, *J. Am. Chem. Soc.*, **98**, 8387 (1976).
(11) L. A. Constant and D. G. Davis, *Anal. Chem.*, **47**, 2253 (1975).

0020-1669/81/1320-1348$01.25/0

Table I. Half-Wave Potentials ($E_{1/2}$, V) of the Fe(III)/Fe(II) Redox Couple for TPPFeX in Selected Solvents

solvent	DN	dielectric const	X = ClO_4^-	Br^-	Cl^-	N_3^-	F^-
$EtCl_2$	0.0	10.7	0.24	−0.19	−0.31	−0.38	−0.47
CH_2Cl_2	0.0	8.9	0.22	−0.21	−0.29	−0.42	−0.50
CH_3NO_2	2.7	35.9	0.10	*d*	*d*	*d*	*d*
PhCN	11.9	25.2	0.20	−0.18[a]	−0.34	−0.39	−0.57
CH_3CN	14.1	37.5	0.11	*d*	*d*	*d*	*d*
PrCN	16.6	20.3	0.13	−0.15	−0.27	−0.33	−0.45
$(CH_3)_2CO$	17.0	20.7	0.09	−0.16[a]	−0.28	−0.34	−0.43
THF	20.0	7.6	0.17	−0.24[a]	−0.34	−0.38	−0.47[a]
DMF	26.6	38.3	−0.05	−0.05	−0.18	−0.25	−0.40
DMA	27.8	37.8	−0.04	−0.05	−0.15	−0.24	−0.36
Me_2SO	29.8	46.4	−0.09	−0.09	−0.10	*c*	−0.09 (−0.40)[b]
py	33.1	12.0	0.15	0.17	0.16 (−0.25)[b]	0.15 (−0.28)[b]	0.16 (−0.46)[b]

[a] Determined from cyclic differential pulse voltammetric data. [b] Second reduction process (see text for details). [c] Two different electrode processes were overlapped. [d] Complex was insoluble in solvent system.

Complexes of TPPFeX, where X = Br^-, N_3^-, and F^- were synthesized by acid hydrolysis of $(TPPFe)_2O$ with the appropriate HX. Typically, 200 mg of $(TPPFe)_2O$ were dissolved in 100 mL of CH_2Cl_2 and extracted against an equal volume of 2 M HX, against an equal volume of H_2O, and evaporated to dryness. The crystalline material was dried in vacuo for 8 h. $TPPFeClO_4$ was prepared by metathesis of TPPFeCl with $AgClO_4$ as per the method of Reed and co-workers.[13] The purity of all porphyrin materials were verified by comparison of their visible spectra with literature spectra.

Twelve different nonaqueous, aprotic solvents were used throughout this study. CH_3NO_2 (Baker Chemicals), Me_2SO (Eastman Chemicals), DMA (Fisher Scientific), and PhCN (Aldrich Chemicals) were received as reagent grade from the manufacturer and were dried over 4-Å molecular sieves prior to use. $EtCl_2$ was purchased from Mallinckrodt. Prior to use, portions were extracted with equal volumes of concentrated H_2SO_4, distilled H_2O, and a 5% KOH solution. The extract was then distilled from P_2O_5 and stored in the dark over activated 4-Å molecular sieves. CH_2Cl_2, obtained from Fisher Scientific as technical grade, was treated in a similar fashion. PrCN was obtained from Aldrich Chemical and was purified by the method of Van Duyne and Reilly.[14] Matheson, Coleman and Bell were the suppliers for CH_3CN and $(CH_3)_2CO$, which were dried over 4-Å molecular sieves prior to use. THF was also supplied by Matheson, Coleman and Bell. This solvent was distilled under N_2 from $LiAlH_4$ immediately prior to use. DMF was treated with 4-Å molecular sieves after purchase from Baker Chemicals. When DMF was obtained from Eastman Chemicals, it was first shaken with KOH, distilled from CaO under N_2, and stored over 4-Å molecular sieves before use.

Results and Discussion

Redox Potentials of Fe(III)/Fe(II). Half-wave potentials were measured for the three "metal-centered" redox reactions of the five TPPFeX complexes in 12 nonaqueous solvents. The values obtained for the reduction of TPPFeX are presented in Table I. As seen from this table, reduction potentials for Fe(III) significantly shift as a function of counterion and solvent. In $EtCl_2$, reduction of TPPFeX becomes much more difficult (by up to 0.71 V) as the counterion varies from the weakly coordinating ClO_4^- to the tightly bound F^-. This indicates preferential stabilization of the Fe(III) species over the Fe(II) species. The iron(III) porphyrin–counterion binding strength increases in the order $ClO_4^- < Br^- < Cl^- < N_3^- < F^-$, and this is reflected in the half-wave potentials. Similar stabilizations of Fe(III) over Fe(II) by the counterion are observed in CH_2Cl_2 and PhCN where the potential difference between the complexes where X = ClO_4^- and X = F^- is 0.72 and 0.77 V, respectively. In the weakly coordinating solvents DMA and DMF, this potential difference has decreased to 0.32 and 0.35 V, respectively. In Me_2SO and py, reduction of TPPFeX is essentially independent of counterion. This invariance of $E_{1/2}$ with changes in X suggests identical reactants and products for all five of the complexes investigated and implies that Me_2SO or py solvent molecules have displaced the counterion from the Fe(III) center. Spectroscopic studies of the reduced complexes in py confirm complexation of Fe(II) by two py molecules. Studies of Fe(III) show that for $TPPFeClO_4$, the counterion is also replaced by two py molecules.[7] For the remaining TPPFeX complexes in py, an equilibrium exists between $TPPFe(py)_2^+$ and TPPFeX or TPPFeX(py). This is evidenced by the cyclic voltammetric data which shows two cathodic reduction peaks for the Fe(III)/Fe(II) couple (Table I) as well as by earlier spectroscopic studies.[7]

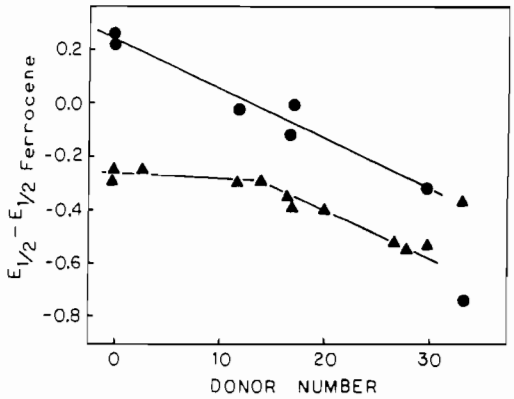

Figure 1. $E_{1/2}$ dependence of the Gutmann donor number for TPPCo and $TPPFeClO_4$. ▲ denotes $TPPFeClO_4$ reduction, and ● denotes $TPPCoClO_4$ reduction.

The effect of solvent on the half-wave potentials for the reduction of $TPPCoClO_4$ has been previously reported.[16,17] In CH_2Cl_2, the Co(III)/Co(II) reaction is observed at 0.69 V. Changing to an aprotic solvent of higher coordinating ability results in a cathodic shift of potential for the metal reaction until, in neat py, a potential of −0.214 V is obtained. This shift can be explained qualitatively as due to preferential axial coordination of Co(III) over Co(II) by solvent molecules acting as ligands.

For determination of the effect of solvent coordination on the half-wave potential, a correlation was attempted with the Gutmann donor number. This empirically determined parameter has proven to be quite useful for intercomparing the potential of a given redox reaction which has been measured in a variety of solvents.[18] For elimination of differences in

(12) A. D. Adler, F. R. Longo, F. Kampas, and J. Kim, *J. Inorg. Nucl. Chem.*, **32**, 2443 (1970).
(13) C. A. Reed, T. Mashiko, S. P. Bentley, M. E. Kastner, W. R. Scheidt, K. Spartalion, and G. Lang, *J. Am. Chem. Soc.*, **101**, 2948 (1979).
(14) R. P. Van Duyne and C. N. Reilley, *Anal. Chem.*, **44**, 142 (1972).
(15) K. M. Kadish, R. K. Rhodes, and L. A. Bottomley, unpublished results.
(16) L. A. Truxillo and D. G. Davis, *Anal. Chem.*, **47**, 2260 (1975).
(17) F. A. Walker, D. Beroiz, and K. M. Kadish, *J. Am. Chem. Soc.*, **98**, 3484 (1976).

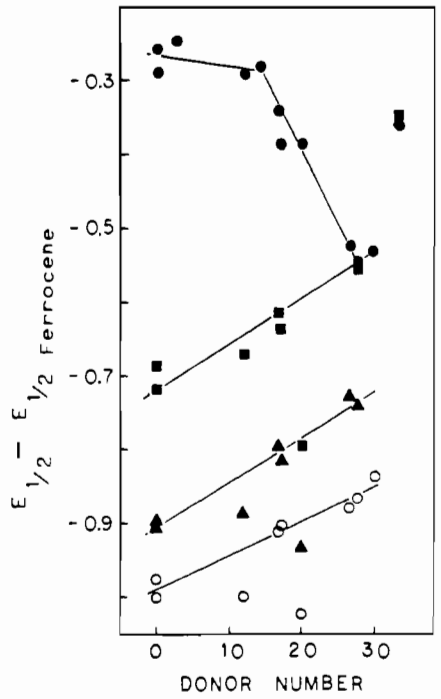

Figure 2. $E_{1/2}$ dependence of the Gutmann donor number for TPPFeX. ● denotes $TPPFeClO_4$, ■ denotes TPPFeBr, ▲ denotes $TPPFeN_3$, and ○ denotes TPPFeF.

liquid junction potential contributions arising between one solvent and another, the potentials have been referenced against the measured value of the ferrocene/ferrocenium ion couple in each solvent.[19]

When the half-wave potentials for $TPPCo^+/TPPCo$ are plotted against the Gutmann donor number (Figure 1), a linear relationship is observed for all solvents except py. The magnitude and direction of the potential shift with solvent indicates a stronger axial coordination of solvent to Co(III) than to Co(II). The $E_{1/2}$ value observed in py is more negative than would be predicted from the $E_{1/2}$–DN relationship.

Plots of $E_{1/2}$ for reduction of $TPPFeClO_4$ vs. donor number were constructed for comparison with $TPPCoClO_4$ and are also shown in Figure 1. In solvents of donicity up to ~15, the potential for reduction of $TPPFeClO_4$ remained essentially constant. This suggests that in these solvents ClO_4^- is bound to the Fe(III) center and that there is only weak or no direct interaction between the solvent and Fe(II). As the solvent donicity increases from 15, the Fe(III)/Fe(II) potential shifts negatively with a slope identical with that observed for $TPPCoClO_4$. py is again an exception to this trend, but with an observed potential 0.25 V more positive than would be predicted. The lack of fit by py to the trends observed for both $TPPCoClO_4$ and $TPPFeClO_4$ may be an inherent property of the donor atom–metal interaction, or it may be due to a change of spin state and/or coordination which is different in this solvent from all of the other solvents investigated. It is unlikely that the observed deviation is due to errors in liquid junction potential correction since the deviations from the predicted potentials are in opposite directions.

On the basis of the similar potential shifts of $TPPCoClO_4$ and $TPPFeClO_4$ with solvent coordinating ability, it can be stated that the Co(III) oxidation state is preferentially stabilized over the Co(II) oxidation state by axial ligands (in this case solvent molecules) and that the Fe(III) oxidation state is stabilized over the Fe(II) oxidation state by the same solvent molecules. This is true, but only when the counterion is ClO_4^-.

Table II. Half-Wave Potentials ($E_{1/2}$, V) of the Fe(II)/Fe(I) Redox Couple for TPPFeX in Selected Solvents

solvent	DN	dielectric const	X = ClO_4^-	Br^-	Cl^-	N_3^-	F^-
$EtCl_2$	0.0	10.7	−1.05	−1.06	−1.06	−1.11	−1.42
CH_2Cl_2	0.0	8.9	−1.06	−1.06	−1.07	−1.06	−1.50
PhCN	11.9	25.2	−1.06	−1.06	−1.09	−1.12	−1.48
PrCN	16.6	20.3	−1.04	−1.03	−1.05	−1.06	−1.09
$(CH_3)_2CO$	17.0	20.7	−1.00	−0.99	−1.02	−1.06	−1.04
THF	20.0	7.6	−1.12	−1.15	−1.18	−1.13	−1.46
DMF	26.6	38.3	−1.03	−1.03	−1.03	−1.04	−1.02
DMA	27.8	37.8	−1.06	−1.05	−1.03	−1.08	−1.08
Me_2SO	29.8	46.4	−1.14	−1.14	−1.14	−1.14	−1.15, −1.39
py	33.1	12.0	−1.50	−1.48	−1.51	−1.48	−1.50

In marked contrast to the effect of solvent on $TPPFeClO_4$ reduction, potentials of TPPFeX reduction, where X = Br^-, Cl^-, N_3^-, and F^-, are shifted in a *positive* potential direction by coordinating solvents. This is depicted in Figure 2. For X = Br^-, N_3^-, and F^-, the most negative potentials occurred in nonbonding solvents (THF excepted) while the most positive redox potential was observed in py. Reversible electron transfers were observed for all cases except in Me_2SO and py (vide infra). The magnitude and direction of the potential shift with solvent indicates a strong stabilization of Fe(II) relative to Fe(III). Stability constant measurements of TPPFe and TPPFeCl bear this out. log β_2 for axial ligand binding to Fe(II) in CH_2Cl_2 is 7.45[20] to 7.8[5] for py and 0.53 for DMF.[20] In contrast, TPPFeCl binds py only weakly and DMF not at all.

It is interesting to note the "anomalous" behavior of TPPFeX in THF (donor number = 20). When X = Br^-, Cl^-, N_3^-, or F^-, the observed potentials are between 100 and 250 mV more negative than would be predicted from Figure 2. Yet the value of $TPPFeClO_4$ reduction in THF is exactly as predicted. This latter point rules out an incorrect estimation of the liquid junction potential in this solvent as a reason for the observed potential difference. One plausible explanation is based on the dual nature of this solvent. THF has the lowest dielectric constant of the solvents investigated yet has a donor number corresponding to moderate coordinating ability. Solvents investigated with similar donicity ($(CH_3)_2CO$ and DMF) have much higher dielectric constants and would tend to facilitate counterion dissociation. A second explanation is that THF coordinates one solvent molecule to the Fe(III) center of TPPFeX where X = Cl^-, Br^-, N_3^-, and F^- but two molecules to TPPFeX when X = ClO_4^-. This would result in a stabilization of Fe(III) over Fe(II) in the former cases. The reactants at the electrode surface would then be either TPPFeX(THF) or $TPPFe(THF)_2^+ClO_4^-$. Displacement of ClO_4^- by THF molecules is likely due to the weak binding of this counterion.

Redox Potentials of Fe(II)/Fe(I). Half-wave potentials for the reduction of TPPFe in 10 solvent systems are presented in Table II. As will be shown later in this paper, Fe(II) may coordinate strong counterions or solvent molecules to form five- and six-coordinate complexes. This coordination will be reflected by a shift of $E_{1/2}$ in a cathodic direction. As seen in Table II, the sensitivity of $E_{1/2}$ for the Fe(II)/Fe(I) couple to counterion depends on the specific solvent. Previous studies on TPPFeCl have suggested that Cl^- dissociates from the Fe center after electron transfer to form $TPPFe^{II}$[11] and that $TPPFe^I$ does not bind axial ligands.[21] Thus, electroreduction

(18) V. Gutmann, "The Donor-Acceptor Approach to Molecular Interactions", Plenum Press, New York, 1978.
(19) J. B. Headridge, "Electrochemical Techniques for Inorganic Chemists", Academic Press, New York, 1969.
(20) D. Brault and M. Rougee, *Biochemistry*, **13**, 4591 (1974).

Table III. Half-Wave Potentials ($E_{1/2}$, V) of the Fe(IV)/Fe(III) Redox Couple for TPPFeX in Selected Solvents

solvent	DN	dielectric const	X = ClO_4^-	Br^-	Cl^-	N_3^-	F^-
$EtCl_2$	0.0	10.7	1.13	1.17	1.17	1.12	1.15
CH_2Cl_2	0.0	8.9	1.11	1.18	1.14	1.08	1.14
PhCN	11.9	25.2	1.13	1.14	1.16	1.13	1.13
CH_3CN	14.1	37.5	1.12	*a*	*a*	*a*	*a*
PrCN	16.6	20.3	1.24	1.14	1.16	1.15	1.10
$(CH_3)_2CO$	17.0	20.7	1.17	1.17	1.17	1.16	

[a] Complex was insoluble in solvent system.

in noncoordinating media would involve a four-coordinate, intermediate-spin reactant, $TPPFe^{II}$, and a four-coordinate product, $[TPPFe^{I}]^-$.

The similarity in observed potentials for the Fe(II)/Fe(I) couple in $EtCl_2$ when X = ClO_4^-, Br^-, and Cl^- suggests dissociation of the halide and identical coordination for the three complexes. However, the shift in potential to a more difficult reduction when X = N_3^- or F^- implies the existence of a five-coordinate $[TPPFe^{II}X]^-$ species. This is indeed the case, as will be shown later in this paper. Similar arguments involving five-coordinate Fe(II) complexes can be made for the electron transfer in CH_2Cl_2, PhCN, THF, and Me_2SO when X = F^-. However, in PrCN, $(CH_3)_2CO$, DMF, and DMA, the potentials of TPPFeF are essentially identical with those of $TPPFeClO_4$ (see Table II), indicating that F^- is not coordinated to the Fe(II) electrode reactant.

In py all TPPFeX complexes give essentially identical Fe(II)/Fe(I) potentials which are shifted negatively with respect to the potentials observed in the other solvents. The donicities of py and Me_2SO are comparable (33.1 and 29.8, respectively), and one would expect similar stabilities of the $TPPFe(py)_2$ and $TPPFe(Me_2SO)_2$ complexes. The proposed existence of a negatively charged $[TPPFeX]^-$ form in Me_2SO and the absence of this species in py may be attributed to the low dielectric of py (12.0 as compared to 46.4 for Me_2SO).

Redox Potentials for Oxidation of Fe(III). Half-wave potentials for the oxidation of TPPFeX are shown in Table III. This reaction may involve oxidation at the metal center to yield an Fe(IV) complex[22,23] or oxidation to yield an Fe(III) cation radical.[24] The actual site of electron transfer is still an object of controversy.[4] As seen from this table, the potentials for the Fe(III) oxidation are essentially invariant with changes in counterion within a given solvent system. Similarly, the Fe(III) oxidation potentials for a given TPPFeX complex are essentially constant in each of the six solvent systems investigated. There is no appreciable shift in potential even though the coordinating ability of the solvent has increased. This behavior suggests that the electron-transfer site is ring centered rather than metal centered. Such an assignment is not in agreement with the results of an extended Hückel calculation describing the molecular orbitals of these systems.[24] Alternative explanations are that oxidation of $TPPFe^{III}X$ involves removal of an electron from a nonbonding orbital or that the process is metal centered, but the relative stabilities of $[TPPFe^{IV}X]^+$-ClO_4^- vs. $TPPFe^{III}X$ are identical with changes in X. Redox potentials alone are insufficient to differentiate among the above.

Reduction Mechanism in DMF. A number of electrochemical studies of iron porphyrins have been undertaken in DMF.[25-29] This solvent was usually chosen because of its good solvating properties for porphyrins and because of its wide potential window, especially for reductions. However, the exact nature of the DMF–porphyrin interaction was not well understood. Kadish and Larson[26] have proposed the existence of a transient species in the Fe(III) to Fe(II) step in eq 1. This

$$[PFe^{III}Cl]^0 \underset{\text{rate controlling}}{\overset{e^-}{\rightleftharpoons}} [PFe^{III}Cl]^- \rightarrow PFe^{II} + Cl^- \quad (1)$$

mechanism was based on changes in heterogeneous rates of electron transfer and was not substantiated. For this paper, a systematic investigation of the electrode mechanism was undertaken in order to determine the mode of interaction between the solvent and the porphyrin and to prove or disprove the proposed transient intermediate, especially with other anions.

A comparison of the Fe(III) reduction potentials measured in DMF (Table I) indicates that $E_{1/2}$ is influenced by the nature of X although to a lesser extent than in CH_2Cl_2 or $EtCl_2$. The difference in potentials between reduction of TPPFeX when X = ClO_4^- and X = F^- is substantially diminished from the difference observed in nonbonding media (350 mV in DMF compared to 710 mV in $EtCl_2$). This decrease could be attributed to an increase in the relative stabilization of Fe(II) vs. Fe(III) from one solvent to another or by changes in the stoichiometry or spin state of the Fe(III) reactants. Brault and Rougee[20] have reported that $TPPFe^{II}$ coordinates only one DMF molecule axially and does so very weakly (formation constant = 6.2 ± 0.3 when measured in benzene). With such a weak axial coordination of Fe(II), the relative stabilization of Fe(II) over Fe(III) is not a plausible explanation for the observed 360-mV difference in reduction potentials between complexes with different counterions in DMF and $EtCl_2$.

When X = ClO_4^- and Br^-, an identical $E_{1/2}$ of −0.05 V is observed. This implies that the counterion has been displaced by solvent molecules as shown in reaction 2 for X = ClO_4^-.

$$TPPFeClO_4 + 2DMF \rightarrow TPPFe(DMF)_2^+ + ClO_4^- \quad (2)$$

In an attempt to verify displacement of ClO_4^- and Br^- by DMF, an electrochemical titration of $TPPFeClO_4$ in CH_2Cl_2 with DMF was performed. Nernstian behavior was observed for the Fe(III)/Fe(II) and Fe(II)/Fe(I) redox couples between 1.00 mM and 1.00 M DMF. Cathodic potential shifts of the Fe(III) and Fe(II) reduction peaks with increasing [DMF] were analyzed according to the classical methods[30] and indicated that Fe(III) was complexed by two molecules of DMF at high DMF concentrations while $TPPFe^{II}$ was axially complexed by only a single DMF molecule. The formation constants for addition of two DMF molecules to Fe(III) according to reaction 2 and one DMF molecule to Fe(II) were 9×10^4 and 2.0, respectively. Clearly, the decrease in potential difference for the Fe(III)/Fe(II) redox couple between X = ClO_4^- and F^- in DMF is not due to differences in the Fe(III)–counterion interaction but is due to the net stability of TPPFeF compared to that of $TPPFe(DMF)_2^+$.

The observed potential for the Fe(III)/Fe(II) couple when Cl^- is the $TPPFe^+$ counterion is midway between X = ClO_4^-

(21) D. Lexa, M. Momenteau, J. Mispeltier, and J. M. Lhoste, *Bioelectrochem. Bioenerg.*, **1**, 108 (1975).
(22) R. H. Felton, G. S. Owen, D. Dolphin, and J. Fajer, *J. Am. Chem. Soc.*, **93**, 6332 (1971).
(23) R. H. Felton, G. S. Owen, D. Dolphin, A. Forman, D. C. Borg, and J. Fujer, *Ann. N.Y. Acad. Sci.*, **206**, 504 (1973).
(24) E. Shimomura, M. Phillippi, and H. Goff, private communication.
(25) K. M. Kadish and L. A. Bottomley, *J. Am. Chem. Soc.*, **99**, 2380 (1977).
(26) K. M. Kadish and G. Larson, *Bioinorg. Chem.*, **7**, 95 (1977).
(27) K. M. Kadish, G. Larson, D. Lexa, and M. Momenteau, *J. Am. Chem. Soc.*, **97**, 282 (1975).
(28) R. Bury and J. Jordan, *Anal. Chem.*, **49**, 1573 (1977).
(29) K. M. Kadish, L. A. Bottomley, and D. Beroiz, *Inorg. Chem.*, **17**, 1124 (1978).
(30) D. R. Crow, "Polarography of Metal Complexes", Academic Press, London, 1969.

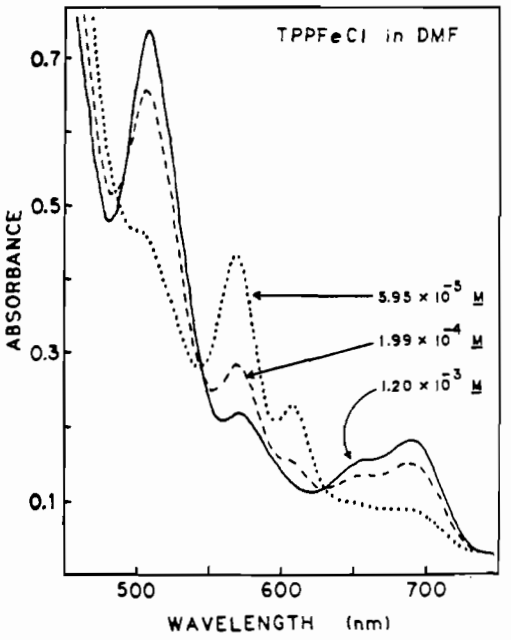

Figure 3. Spectral changes as a function of [TPPFeCl] in DMF (0.1 M TBAP).

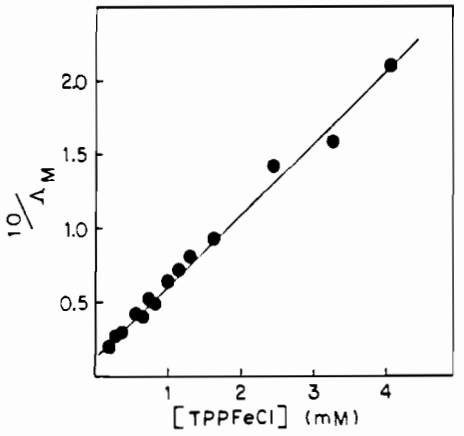

Figure 4. Molar conductance of TPPFeCl as a function of concentration in DMF.

and F^-. Association of Cl^- in our electrochemical experiments was verified spectrophotometrically. Figure 3 depicts the spectral changes observed as a function of [TPPFeCl] in DMF. The data are displayed such that the product of concentration of TPPFeCl times the optical path length is a constant at all concentrations of TPPFeCl. At 1.20×10^{-3} M TPPFeCl, the spectrum in DMF is essentially identical with that observed in CH_2Cl_2 or $CHCl_3$.[31] As the [TPPFeCl] is decreased, spectral data indicate chemical transformations in the chromophore. At 5.95×10^{-5} M TPPFeCl, the observed spectrum is very similar to that obtained in Me_2SO. The halide is associated in CH_2Cl_2 and completely dissociated in Me_2SO.[32]

Dissociation of the Cl^- at lower [TPPFeCl] was confirmed from conductance studies. At electrochemical concentrations of TPPFeCl (~1 mM), the porphyrin behaves essentially as a nonelectrolyte. As the concentration is decreased, the molar conductance increases. The reciprocal of the measured molar conductance was plotted against [TPPFeCl] and is depicted in Figure 4. The linear trace indicates that TPPFeCl is actually a weak electrolyte. From the data, an association

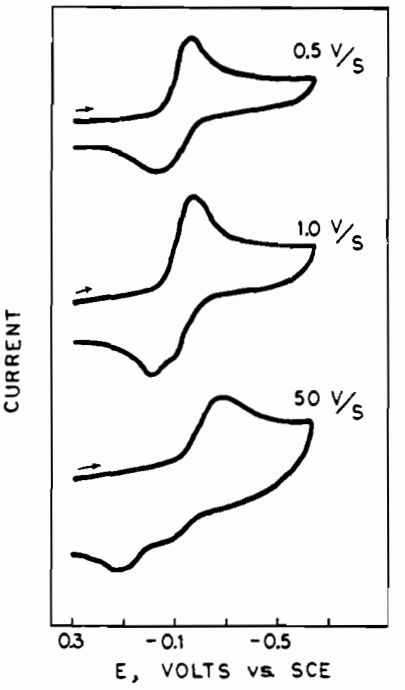

Figure 5. Cyclic voltammograms of TPPFeCl in DMF at selected scan rates.

constant (as defined in eq 3) was calculated as $K_a = 4.0 \times 10^3$ with $\Lambda_0 = 83\ \Omega^{-1}\ cm^{-1}$.

$$TPPFe(DMF)_2^+ + Cl^- \rightarrow TPPFeCl + 2DMF \quad (3)$$

Figure 5 shows cyclic voltammograms obtained for the Fe(III)/Fe(II) couple of TPPFeCl in DMF. On the negative potential sweep, only one cathodic process is observed while on the reverse sweep, one or two peaks are observed, depending upon the rate of potential scan. At slow scans, one broadened anodic process is observed. Addition of Cl^- in the form of TBACl causes a decrease in peak width similar to that observed for TPPFeBr and TPPFeCl in nonbonding media (see later sections). As the scan rate is increased the one broad anodic process splits into two processes. The oxidation peak at more positive potentials is essentially identical with that obtained when the starting material is $TPPFeClO_4$. Current–voltage curves similar to those depicted for Cl^- are obtained when X = N_3^- and F^-.

Nicholson and Shain[33] strategies and variable-temperature electrochemistry were employed to evaluate any equilibrium in solution and to detect possible reactions coupled to the electron transfer. The Nicholson–Shain strategy includes variation in potential scan rates and measurements of both peak potentials and peak currents as a function of scan rate.

Experimentally obtained slopes of 30 mV cathodic shift with tenfold increase in scan rate for TPPFeX where X = Cl^-, N_3^-, or F^- agree with the predicted values[33] for the case of a rapid chemical reaction following the electron transfer. When X = ClO_4^- or Br^- the reactant is $TPPFe(DMF)_2^+$, and reversible electron transfers without coupled chemical reactions are obtained. When X = Cl^-, N_3^-, or F^-, the reactant is either TPPFeX or TPPFeX(DMF). The exact stoichiometry cannot be unambiguously assigned on the basis of the available spectrophotometric and electrochemical data. In either case, the reduction step generates $[TPPFeX]^-$ which readily dissociates to form the ultimate product, TPPFe(DMF). That

(31) F. A. Walker, M. W. Lo, and M. T. Ree, *J. Am. Chem. Soc.*, **98**, 5552 (1976).
(32) S. B. Brown and I. R. Lantzke, *Biochem. J.*, **115**, 279 (1969).
(33) R. S. Nicholson and I. Shain, *Anal. Chem.*, **36**, 706 (1964).
(34) H. A. Benesi and J. H. Hildebrand, *J. Am. Chem. Soc.*, **71**, 2703 (1949).

Scheme I

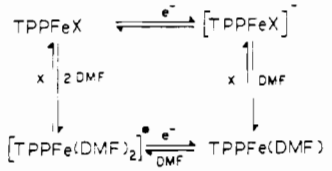

TPPFe(DMF) is the ultimate product in DMF is also shown from the current–voltage curves of $TPPFeN_3$ obtained at several temperatures. At 298 K TPPFe(DMF) converts to $[TPPFeN_3]^-$ before reoxidation and a reversible C–V curve is obtained. Lowering of the temperature slows reassociation of the anion and direct oxidation of TPPFe(DMF) proceeds at $E_{p,a} = -0.08$ V, a potential almost identical with that observed for $TPPFeClO_4$ in the same solvent. At 215 K reoxidation via $[TPPFeN_3]^-$ has decreased to a negligible amount, and almost all oxidation is from TPPFe(DMF) directly to $TPPFe(DMF)_2^+$.

A summary of the mechanism for all complexes of TPPFeX in DMF is shown in Scheme I. At rapid scan rates or low temperatures, oxidation of TPPFe(DMF) can proceed via two different pathways, i.e., directly to $TPPFe(DMF)_2^+$ or via $[TPPFeX]^-$ to TPPFeX. Each of these processes has a characteristic half-wave potential and accounts for the two anodic peaks observed at high scan rates and low temperatures. At slow scan rates or high temperatures, however, TPPFe(DMF) has time to interconvert to $[TPPFeX]^-$ prior to the electron transfer and is oxidized by the thermodynamically easier path (most negative potential). Likewise, addition of free X shifts the equilibrium toward $[TPPFeX]^-$. This chemical reaction causes the apparent coalescence of the two anodic process observed at high scan rates. The driving force is the ease with which $[TPPFeX]^-$ can be oxidized with respect to TPPFe(DMF).

Reactions in Me_2SO. Reduction of $TPPFeN_3$. For X = ClO_4^-, Br^-, and Cl^-, superimposable cyclic voltammograms were obtained for each of the three reduction steps. The electrode reaction occurring at −0.09 V corresponded to the Fe(III)/Fe(II) redox couple, at −1.14 V to the Fe(II)/Fe(I) redox couple, and at −1.67 V to the formation of the anion radical.[29] The superimposability of these voltammograms implies identical reactants and products at the electrode surface, which are $TPPFe(Me_2SO)_2^+$ and $TPPFe(Me_2SO)_2^{2+}$. This is confirmed by spectroscopic and conductometric results[32] which indicate dissociation of the counterion in this solvent system.

In contrast to complexes containing ClO_4^-, Br^-, or Cl^-, the voltammogram of $TPPFeN_3$ dissolved in Me_2SO indicates the presence of more than one Fe(III) form in solution. Two cathodic reduction peaks are observed at −0.13 and −0.25 V. The first reduction peak is at an identical potential to that of the Me_2SO bisadduct, while the second more cathodic peak is at a potential suggesting the axial complexation of $TPPFe(Me_2SO)_2^+$ with N_3^-. All other oxidation and reduction potentials were identical with those for the other complexes of TPPFeX where X = Cl^-, Br^-, and ClO_4^-.

The stoichiometry of each Fe(III) species was determined by titration of 1.0 mM TPPFeCl in Me_2SO with NaN_3. Throughout the titration, the ionic strength of the solution was maintained at 0.1 M by appropriate adjustment of [TBAP]. Prior to addition of NaN_3, a single reduction process was observed for the Fe(III)/Fe(II) couple at $E_{p,c} = -0.13$ V. At $[NaN_3]$ less than 1.0 mM, a second peak was observed at $E_{p,c} = -0.25$ V. The current of the second peak increased with increasing $[NaN_3]$. The process at $E_{p,c} = -0.13$ V decreased with increasing $[NaN_3]$ until it completely disappeared at $[NaN_3]$ greater than or equal to 2.0 mM. Increasing the $[NaN_3]$ up to 0.05 M resulted in potential shifts which corresponded to one more N_3^- being bound to the reactant than to the product of the electron-transfer step. On the basis of this result and the potential data for the Fe(II)/Fe(I) couple, the Fe(III) reactants are proposed to be $TPPFe(Me_2SO)_2^+$ and either $TPPFeN_3$ or $TPPFeN_3(Me_2SO)$, respectively. The latter two species are indistinguishable from the available spectroscopic and electrochemical data.

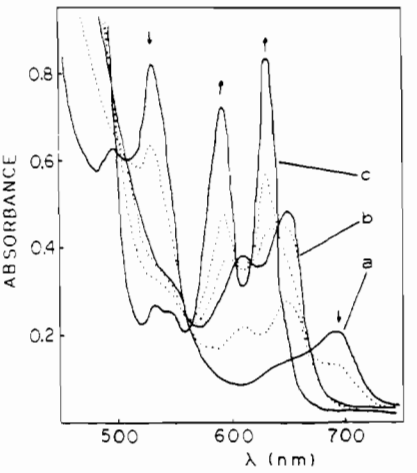

Figure 6. Spectrophotometric titration of $TPPFe(Me_2SO)_2^+$ with TBAF. $[TPPFe(Me_2SO)_2^+] = 6.23 \times 10^{-5}$ M, solvent media = Me_2SO (0.1 M TBAP), [TBAF] = (a) 0.00 M, (b) 1.00×10^{-4} M (F^- monoadduct), and (c) 1.44×10^{-2} M (F^- diadduct).

Reactions in Me_2SO. Reduction of TPPFeF and $TPPFeF_2^-$. The identity of both F^- mono- and diadducts of $TPPFe^+$ were elucidated from spectrophotometric and electrochemical titrations of $TPPFe(Me_2SO)_2^+$ with TBAF. Figure 6 depicts the changes observed in optical absorption spectra during the spectrophotometric titration of $TPPFe(Me_2SO)_2^+$ with F^-. Seven isosbestic points were observed during the course of the titration. At F^- to porphyrin ratios less than 1.7 absorption peaks at 531 and 690 nm decreased proportionately with the increase of peaks at 610 and 649 nm. Isosbestic points were observed at 510, 561, and 670 nm, indicating two distinct species in solution. At high $[F^-]$ the peaks at 610 and 649 nm decreased in intensity and new peaks at 590 and 631 nm grew. Isosbestic points were now observed at 564, 603, 616, and 640 nm, again indicating only two species in solution, but one species which was not present at low $[F^-]$. The spectrum at low F^- concentration was identical with that obtained by dissolving TPPFeF directly in Me_2SO and is proposed to be that of $TPPFeF(Me_2SO)$.

Comparison of the visible spectrum of TPPFeF in Me_2SO with that previously reported by Cohen[35] for both the α and β form of TPPFeF dissolved in CH_2Cl_2 shows striking similarities. Cohen reports absorption maxima at 645, 610, and 550 nm. The spectrum depicted in Figure 6 has maxima at 649 and 610 and a shoulder at 544 nm. Using the 610-nm peak as the reference, Cohen reports the relative peak absorptivities of 0.87 and 0.92 for the 645- and 550-nm peaks, respectively. The relative peak absorptivities observed in Me_2SO are 1.28 and 0.86 for the 649- and 544-nm peaks, respectively. This implies a substantial interaction by the solvent which can be explained by either solvent–solute interaction at the porphyrin π system or by direct axial coordination of the Fe center by a Me_2SO molecule. On the basis of the existence of other unsymmetrically substituted complexes (e.g., TPPFe(CN)py),[36] the $TPPFeF(Me_2SO)$ species

(35) I. A. Cohen, D. A. Summerville, and S. R. Su, *J. Am. Chem. Soc.*, **98**, 5813 (1976).
(36) J. Del Gaudio and G. N. LaMar, *J. Am. Chem. Soc.*, **98**, 3014 (1976).

Scheme II

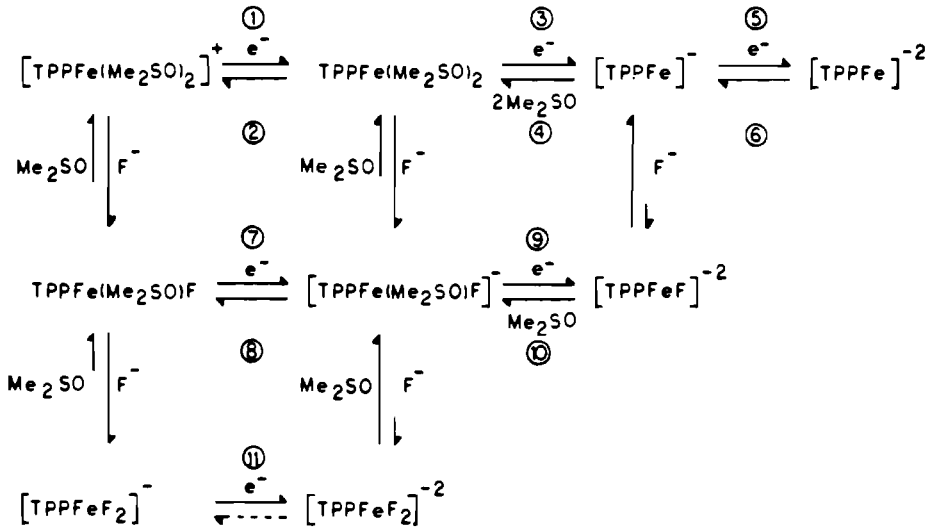

is the proposed formulation of the F^- monoadduct. The stoichiometry of the final chromophore was evaluated by using the method of Benesi and Hildebrand.[34] Analysis of the data at 531, 590, and 631 nm indicates 1.93 molecules of F^- per molecule of $TPPFe(Me_2SO)_2^+$. The identification of a F^- diadduct is not novel for the heme system. Momenteau and co-workers[37] have identified a F^- diadduct of deuterohemin IX dimethyl ester using visible and ESR spectroscopic techniques. However, the stoichiometry of the F^- monoadduct is of some interest. Recent work by Scheidt and co-workers[38] as well as by Bottomley et al.[7] has demonstrated the existence of unsymmetrically substituted six-coordinate iron(III) porphyrins in which py was trans to the N_3^- counterion.

A cyclic voltammogram of TPPFeF in Me_2SO is displayed in Figure 7b. Five separate electrode reactions were observed at $E_{1/2}$ = −0.09, −0.40, −1.15, −1.39, and −1.63 V, respectively. The redox couples at −0.09, −1.15, and −1.63 V (labeled peaks 1–6) are identical with potentials observed for reduction of TPPFeCl, TPPFeBr, $TPPFeClO_4$, and $TPPFeN_3$ and have been discussed in the previous section. The reactions at $E_{1/2}$ = −0.40 (peaks 7 and 8) and −1.39 V (peak 9) correspond to reductions of Fe(III) and Fe(II) complexes which are axially complexed by F^- ion. Evidence for a F^- monoadduct is derived directly from the electrochemical results. $TPPFe(Me_2SO)_2^+$ was titrated with F^-, and the current–voltage curves were recorded as a function of F^- concentration. At F^- to porphyrin ratios greater than zero but less than 3.0, the voltammograms obtained were qualitatively similar to that depicted in Figure 7b for TPPFeF in Me_2SO. As $[F^-]$ was increased, the relative currents for the processes at −0.40 and −1.39 V increased directly with a proportional decrease in current of the −0.09- and −1.15-V processes. At F^- to porphyrin ratios greater than 3.0, the cathodic process at −0.40 V decreased in current until it completely disappeared in the background at a mole ratio of 6.0. A new cathodic process at $E_{p,c}$ = −1.15 V grew proportionately.

A typical cyclic voltammogram at high $[F^-]$ is shown in Figure 7c. The oxidation process labeled as peak 8 has a potential identical with that of process observed at low $[F^-]$ or in the absence of added F^-. This process is coupled to the reduction at −1.15 V (peak 11, Figure 7c). Both peak 8 and peak 11 gave shape geometries as well as current–potential sweep rate relationships consistent with a chemical reaction

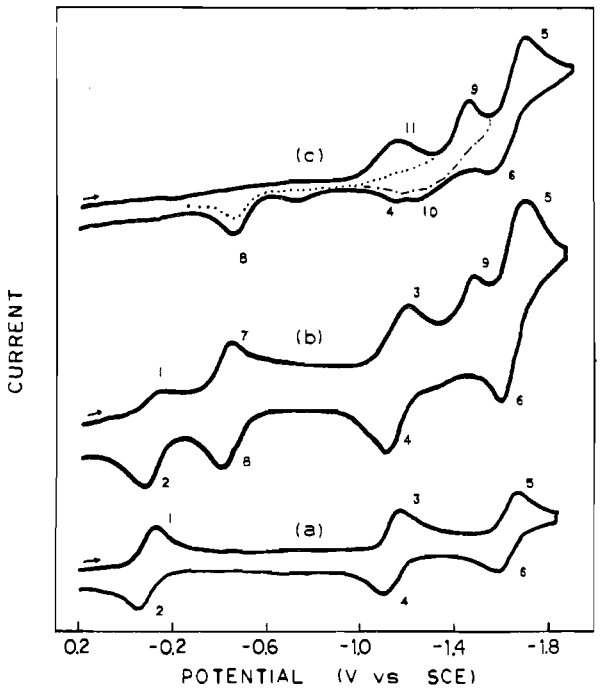

Figure 7. Cyclic voltammograms of (a) $TPPFe(Me_2SO)_2^+$, (b) TPPFeF, and (c) $TPPFeF_2^-$ in Me_2SO (0.1 M TBAP). Scan rate = 0.50 V/s.

following the electron-transfer step.[33] Peak 9 is similar in shape to and identical in potential with the reduction process observed at low $[F^-]$ (Figure 7b). This suggests an identical coordination of $TPPFeF^-$ at high and low $[F^-]$ and that there is no change in coordination upon reduction of Fe(II). However, the lack of a well-defined reverse peak (see peaks 4 and 10 in Figure 7c) indicates that the product of the electron transfer is not stable on the cyclic voltammetric time scale.

On combination of both the spectroscopic and electrochemical titration results, the overall electrode mechanisms depicted in Scheme II are proposed. The numbers in the scheme correspond to the anodic and cathodic peaks which are labeled in Figure 7.

In the absence of F^- the reduction–oxidation process is via the top sequence of steps 1–6. At molar ratios of F^- to porphyrin less than 6.0, the primary reactant at the electrode is $TPPFe(Me_2SO)F$ which is in equilibrium with $TPPFe(Me_2SO)_2^+$. The former species is reduced to $[TPPFe(Me_2SO)F]^-$ (peak 7) which exists in equilibrium with

(37) D. Lexa, M. Momenteau, and J. Mispelter, *Biochim. Biophys. Acta*, **338**, 151 (1974).
(38) K. M. Adams, P. G. Rasmussen, W. R. Scheidt, and K. Hatanto, *Inorg. Chem.*, **18**, 1892 (1979).

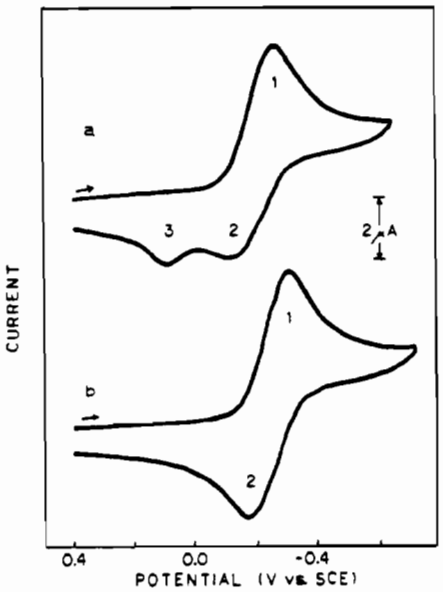

Figure 8. Cyclic voltammograms of TPPFeBr in CH_2Cl_2 as a function of supporting electrolyte: (a) 0.1 M TBAP; (b) 0.09 M TBAP, 0.01 M TBABr. Scan rate = 0.100 V/s.

$TPPFe(Me_2SO)_2$. The iron(II) porphyrin is stabilized with F^- complexation as evidenced by the additional energy required to reduce the resultant complex (peak 9 vs. 3 in Figure 7). Reduction to the Fe(I) species produces the uncomplexed $[TPPFe]^-$ complex even though a transient $[TPPFeF]^{2-}$ species is indicated from the electrochemical data. At all concentrations of F^-, the anion radical (peaks 5 and 6) is unaffected by F^-. At higher molar ratios of F^- to porphyrin, the F^- diadduct of Fe(III), $TPPFeF_2^-$, is predominant in solution as well as the F^- monoadduct of Fe(II), $[TPPFe(Me_2SO)F]^-$.

Reduction Mechanism in Nonbonding Solvents. CH_2Cl_2 and $EtCl_2$. Three different pathways for electron transfer were observed in CH_2Cl_2 (or $EtCl_2$) as a function of the counterion bound to the iron center. When $X = ClO_4^-$, three reversible electron transfers were obtained which, for Fe(III) reduction, corresponded to the electrode reaction in eq 4. When X =

$$TPPFeClO_4 \overset{e^-}{\rightleftharpoons} TPPFe + ClO_4^- \qquad (4)$$

N_3^- or F^-, three reversible reactions were again obtained. In this case, however, Fe(III) reduction proceeded according to eq 5 at −0.38 to −0.50 V. The reduction product, $[TPPFeX]^-$,

$$TPPFeX \overset{e^-}{\rightleftharpoons} [TPPFeX]^- \qquad (5)$$

is not a transient intermediate, and discrete five-coordinate Fe(II) complexes may be obtained. This has been discussed in detail for the case of TPPFeF. When $X = Cl^-$ or Br^-, coupled chemical reactions were observed and the reduction–reoxidation sequence involved a combination of pathways 4 and 5. This is illustrated by the cyclic voltammogram of TPPFeBr shown in Figure 8. Reduction of TPPFeBr in 0.1 M TBAP results in a single reduction peak corresponding to reaction 5 and two oxidation peaks corresponding to reaction 4 and 5. That $[TPPFeBr]^-$ is the product of the reduction is confirmed by titration of TPPFeBr with excess Br^-. Increasing the concentration of Br^- in solution while keeping the ionic strength of the solution constant resulted in the disappearance of peak 3 (shown in Figure 8b). Multiple scans under the conditions of high Br^- concentration (Figure 8) showed only one reduction process (peak 1). This indicated that there is no appreciable dissociation of TPPFeBr in bulk and that the equilibrium between $TPPFeClO_4$ and TPPFeBr favors the latter species. Results similar to those for TPPFeBr were obtained for TPPFeCl in CH_2Cl_2 and have been presented previously when the solvent was $EtCl_2$.[7]

Scheme III

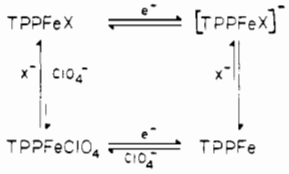

A summary of the three-electron transfer sequences for TPPFeX reduction is given in Scheme III. When $X = ClO_4^-$ the bottom pathway is followed. This is the easier reduction in the series, and $E_{1/2}$ for Fe(III)/Fe(II) is determined by the stability of the $TPPFe^+$–ClO_4^- interaction.[39] When $X = N_3^-$ or F^-, the top electron-transfer path in Scheme III is followed. No appreciable dissociation of $[TPPFeX]^-$ occurs and reversible electron transfers are obtained. The half-wave potentials for these reactions are the most cathodic of the series, and the reductions are the most difficult. It is significant to note that, for these complexes, the half-wave potentials are influenced by the relative stabilities of the iron(III) *and* iron(II) halide interaction. Increases in the Fe(III) bond strength result in a cathodic shift of $E_{1/2}$ while increases in the Fe(II) bond strength shift potentials in the opposite direction. The 720-mV stabilization of TPPFeF when compared to that of $TPPFeClO_4$ thus corresponds to a 10^{12} increase in stabilization of reaction 5 over reaction 4. Individual Fe(III) stabilization by F^- is substantially greater than 10^{12} when compared to ClO_4^- but has not been measured.

In summary, it should be stated that the proposed "box" mechanism in Scheme III is restricted to noncoordinating solvents with TBAP as the supporting electrolyte. Substitution of TBAP by either $TBAPF_6$ or $TBABF_4$ yielded two processes for the Fe(III)/Fe(II) reaction. The easier reduction occurs at 0.22 V and is indicative of $TPPFe^+$ reduction with either ClO_4^-, PF_6^-, or BF_4^- as the associated counterion. The more cathodic potential is at −0.50 V and is reminiscent of the reduction of TPPFeF. The absolute currents for the more cathodic peak increased as a function of time with a proportionate decrease in the anodic peak currents. These results indicate that PF_6^- or BF_4^- was dissociating to form PF_5 or BF_3 and F^-. The driving force for the dissociation reaction is presumed to be the net stabilization of TPPFeF by up to 0.72 V when compared to $TPPFePF_6$, $TPPFeBF_4$, or $TPPFeClO_4$.

Solvent–Counterion Interactions. It is clear from the data presented in this paper that half-wave potentials for TPPFeX reduction will depend on the nature of the counterion and the donicity of the solvent. The type of counterion associated with Fe(III) and Fe(II) is the predominant factor governing the type of electron-transfer mechanism observed for electroreduction of iron porphyrins. In a nonbonding solvent, the redox potential of the Fe(III)/Fe(II) couple can be "tuned" over a 720-mV potential range by appropriate selection of the Fe(III) counterion. This range, as well as the stoichiometry of both the electrode reactant and product, can be modified by changing the solvent in which the redox reactions are carried out.

Despite the knowledge gained from this study, it is still difficult to quantitate the individual effects of solvent and counterion separately. For a complete understanding of the influence of each factor, the electrode mechanism must be

(39) Identical potentials have been obtained when the initial complex was $TPPFeBF_4$, $TPPFePF_6$, or $TPPFeClO_4$ or when $TBAPF_6$ or $TBABF_4$ are used as supporting electrolytes with $TPPFeClO_4$. On the basis of this, it has been stated in the literature that the potential of 0.22–0.24 V is for reduction of the free ion. However, NMR and conductivity studies in CH_2Cl_2 show that $TPPFeClO_4$ is not a 1:1 electrolyte and is fully associated.

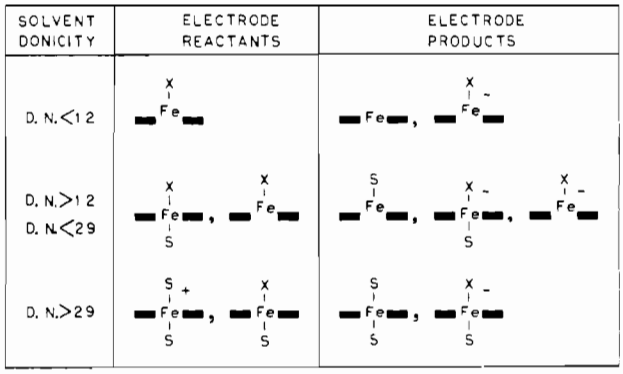

Figure 9. Summary of overall electron-transfer schemes.

clearly defined in each solvent. A general redox mechanism which shows counterion and solvent association to Fe(III) and Fe(II) is shown in Figure 9. In solvents of donor number less than 12, the electrode reactant is TPPFeX which may be reduced to either $[TPPFeX]^-$ (reaction 5) or TPPFe (reaction 4) depending on the nature of X. In donor number solvents between 12 and 29, the reactant is either TPPFeX or TPPFeX(S) which is reduced to either $[TPPFeX]^-$, TPPFeS, or $[TPPFeX(S)]^-$. These products may be transient intermediates depending on the nature of X and can convert to TPPFe(S) as the ultimate product. This has been shown in detail for the reactions in DMF. In solvents with a donor number greater than 29 (such as py), solvent bisadducts as well as the mixed-ligand adducts are formed for both the reactant and product.

Potential–Spin State Dependencies. Finally, the question of the dependence of Fe(III) and Fe(II) spin state on the redox potential must be considered. Iron porphyrins complexes may be four-, five-, or six-coordinate in solution and will contain either high-, intermediate-, or low-spin Fe depending upon the type of axial ligand. All six-coordinate iron porphyrin complexes with nitrogenous bases have been identified as being low spin,[40] whereas all six-coordinate complexes with oxygen donor ligands are high spin.[41] The intermediate-spin state has been assigned in solution to both Fe(III) and Fe(II) when the porphyrin was dissolved in nonbonding, aprotic media. For Fe(II), this implies a vacant fifth and sixth axial positions.[20] For Fe(III) with weakly coordinating anions (e.g., TPPFeX where X = ClO_4^-, BF_4^-, or PF_6^-) an admixture of $S = {}^3/_2$, ${}^5/_2$ has been assigned to the system.[42,43] Low-spin pentacoordinate complexes have rarely been observed.[44] In contrast, high-spin Fe(III) complexes are formed when the counterion X is either a halide or a strong field anion (e.g., N_3^-).[2] High-spin porphyrin complexes of Fe(II) are also formed when a sterically hindered nitrogenous base occupies the fifth coordination site.[45]

When all possible spin states of each reactant and product are considered, nine types of electron-transfer reactions are possible. These are high-spin Fe(III) reduced to high-, intermediate-, or low-spin Fe(II); intermediate-spin Fe(III) reduced to high-, intermediate-, or low-spin Fe(II); and low-spin Fe(III) reduced to high-, intermediate-, or low-spin Fe(II). Five of these nine possibilities may be eliminated on the basis of the known chemistry of the iron porphyrin systems. If we assume that electron transfer between redox species of different spin multiplicites is spin forbidden,[46] or at least spin restricted, we can exclude one of the remaining four which is high-spin Fe(III) reduced to intermediate-spin Fe(II). This leaves three electrode reactions (eq 6–8) which exist in the iron porphyrin

$$Fe(III)_{HS} \rightleftharpoons Fe(II)_{HS} \quad (6)$$

$$Fe(III)_{IS} \rightleftharpoons Fe(II)_{IS} \quad (7)$$

$$Fe(III)_{LS} \rightleftharpoons Fe(II)_{LS} \quad (8)$$

systems. HS, IS, and LS represent the high-, intermediate-, and low-spin forms of the iron, respectively.

Table IV. Dependence of $E_{1/2}$ on Spin State for Reduction of Various Complexes of $TPPFe^{III}$

spin-state change	electrode reaction	$E_{1/2}$, V	ref
LS → LS	$TPPFe(pyX)_2^+ \rightleftarrows TPPFe(pyX)_2$	+0.31 to −0.17	*c*
	$TPPFe(Im)_2^+Cl^- \rightleftharpoons TPPFe(Im)_2$	−0.115	*d*
	$TPPFeF_2^- \rightleftarrows TPPFeF_2^{2-}$	−1.10	this work, *b*
IS → IS	$TPPFeClO_4 \rightleftarrows TPPFe$	+0.17	this work
HS → HS	$TPPFeX \rightleftarrows [TPPFeX]^-$	−0.19 to −0.57	this work
	$TPPFe(Me_2SO)_2^+ \rightleftharpoons TPPFe(Me_2SO)_2$	−0.09	this work

[a] Measured in CH_2Cl_2, except where noted. [b] Measured in Me_2SO (0.1 M TBAP). [c] Reference 9. [d] Measured in DMF (0.1 M TBAP).[21]

A summary of the half-wave potentials observed in this study as well as potentials in the literature as a function of Fe(III) and Fe(II) spin state are given in Table IV. Reduction of $TPPFeClO_4$ in nonbonding media involves an intermediate-spin Fe(III) reactant and Fe(II) product. Substitution of ClO_4^- by Br^-, Cl^-, N_3^-, or F^- yields a high-spin reactant. Reduction of TPPFeBr or TPPFeCl yields as initial product the high-spin $[TPPFeX]^-$. Reduction of $TPPFeN_3$ or TPPFeF yields predominantly the high-spin Fe(II) product, $[TPPFeN_3]^-$, or $[TPPFeF]^-$. As seen in Table I and Figure 2, the intermediate-spin Fe(III) complexes are reduced at 0.17 ± 0.06 V. The low-spin $TPPFe(py)_2^+$ complex is also reduced at 0.15 V. High-spin TPPFeX or $TPPFeS_2^+$ complexes (where S = DMF, Me_2SO, etc.) are reduced from −0.05 to −0.57 V. Yet, the low-spin $TPPFe(4\text{-}Me_2Npy)_2^+$ complex is reduced at −0.17 V,[5] well within the range listed for high-spin complexes.

When the initial reactant is TPPFeBr, $TPPFeClO_4$ or TPPFeCl, the ultimate Fe(II) complex is the intermediate-spin TPPFe. The potential for reduction of this complex to $[TPPFe^I]^-$ is −1.04 ± 0.02 V in nonbonding media. As seen in Table II, reduction potentials of the high-spin complexes $[TPPFeN_3]^-$ and $[TPPFeF]^-$ are cathodically shifted by up to 360 mV from that observed for the intermediate-spin complex TPPFe. A similar cathodic potential shift is observed for reduction of $TPPFe(py)_2$, a low-spin complex. Thus, both the high-spin, five-coordinate, and low-spin, six-coordinate, Fe(II) complexes are more difficult to reduce than the four-coordinate, intermediate-spin, Fe(II) form. This reflects the stability of the Fe(II) mono- and bisadducts over the uncomplexed TPPFe rather than the influence of spin state on the redox potential. Clearly, there is no straightforward relationship between the observed Fe(III)/Fe(II) or Fe(II)/Fe(I) potential on the Fe(III) or Fe(II) spin state. Rather, the axial coordination of both the Fe(III) and Fe(II) centers by nitrogenous bases, solvent molecules, and/or monovalent anions

(40) W. R. Scheidt, *Acc. Chem. Res.*, **10**, 339 (1977).
(41) C. A. Reed, T. Mashiko, S. P. Bentley, M. E. Kastner, W. R. Scheidt, K. Spartalion, and G. Lang, *J. Am. Chem. Soc.*, **101**, 2948 (1979).
(42) H. Goff and E. Shimomura, *J. Am. Chem. Soc.*, **102**, 31 (1980).
(43) D. H. Dolphin, J. R. Sams, and T. B. Tsin, *Inorg. Chem.*, **16**, 711 (1977).
(44) W. R. Scheidt and M. E. Frisse, *J. Am. Chem. Soc.*, **97**, 17 (1975).
(45) D. Brault and M. Rougee, *Biochem. Biophys. Res. Commun.*, **57**, 654 (1974).
(46) H. Yasuda, K. Suga, and S. Aoyagui, *J. Electroanal. Chem.*, **86**, 259 (1975).

controls the observed redox potential.

Acknowledgment. The authors wish to thank the National Institutes of Health (Grant No. GM 2517-02) and the Robert A. Welch Foundation (Grant No. E-680) for support of this work. The help of Dwight Schaeper in doing the variable-temperature electrochemistry of $TPPFeN_3$ is appreciated. The assistance of Dr. Kamelendu Das and Dwight Schaeper in synthesizing $TPPFeClO_4$ is also acknowledged.

Registry No. $TPPFeClO_4$, 57715-43-2; TPPFeBr, 25482-27-3; TPPFeCl, 16456-81-8; $TPPFeN_3$, 51455-98-2; TPPFeF, 55428-47-2; $TPPCoClO_4$, 76402-67-0; $TPPFeF_2^-$, 76402-68-1; $TPPFe(Me_2SO)_2^+$, 68179-07-7.

Contribution from the General Electric Corporate Research & Development Center, Schenectady, New York 12301

Transition-Metal Photocatalysis: Rhodium(I)-Promoted Hydrosilation Reactions

ROBERT A. FALTYNEK

Received September 12, 1980

Rhodium(I) complexes were found to be active photocatalyst precursors for the hydrosilation reaction. Substrates studied included Si–H and Si–vinyl functionalized siloxanes as well as simple terminal alkenes. Reaction rates dramatically increased when the mixtures were photolyzed in the presence of air or soluble oxidizing agents. Near-UV irradiation enhanced dissociation of the catalyst precursors and promoted oxidation of dissociated phosphine or phosphite ligands in $ClRh(O_2)(PPh_3)_3$ and the complexes formed between $RhCl_3 \cdot 3H_2O$ and PBu_3, $P(OEt)_3$, and $P(OBu)_3$. Efficiency of $ClRh(PPh_3)_2$ formation was shown to be the rate-determining criterion in the oxidized Rh–PPh_3 system. The positive oxygen dependence and unequivocally photocatalytic nature of hydrosilation in the presence of the Rh(I) compounds are unprecedented in Si–H addition catalysis. The previously studied $Fe(CO)_5$ hydrosilation catalysts are completely inactive in air, and even in vacuo the lifetime of the active iron species subsequent to irradiation is exceedingly short compared to that of the Rh(I) intermediates described here.

Introduction

The activation of alkenes toward addition and isomerization reactions by transition-metal complexes has received considerable attention in the recent literature.[1] Studies on metal-catalyzed hydrogenation, hydroformylation, and hydrosilation have defined a common ground between diverse areas of chemistry. Furthermore, since these reactions are crucial to process chemistry, such studies have created a useful interface between academia and industry.

Metal complexes in excited states can often decay via ligand extrusion or bond scission to produce reactive catalytic species otherwise unobtainable under ambient conditions.[2] The ground-state precursors to these intermediates may be classified as photoassistance or photocatalytic agents depending on their activity subsequent to irradiation. Photoassistance agents require continuous irradiation to maintain a catalytically viable species, while true photocatalysts produce thermally active decay products that continue to turn over substrate in the dark following initial irradiation. Even though many classes of low-valent transition-metal complexes and organometallics are photochemically active upon near-ultraviolet excitation, there has been surprisingly little work done in the area of light-generated catalysts.[3]

Practically all of the literature reports on photoinduced alkene chemistry deal with binary metal carbonyls and their simple substitution products as catalyst precursors.[4–15] Loss

Scheme I

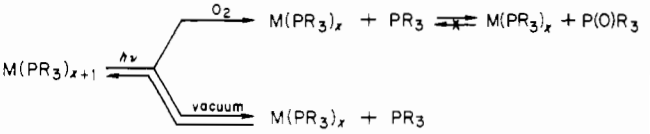

of CO from these complexes is almost 100% efficient upon irradiation into the appropriate ligand field bands. Other low-valent metal compounds containing noncarbonyl ligands also exhibit d–d transitions in the near-UV, and they should at least in theory give rise to similar photodissociative chemistry. Preferential loss of the nitrogen ligand from $M(CO)_5L$ has been observed with good quantum efficiency for various mixed carbonyl–amine group 6B complexes,[16,17] and it was very recently shown that $W[P(OMe)_3]_6$ readily dissociates under mercury-lamp irradiation.[18]

When the labilized ligand is a phosphine or phosphite and the reaction is conducted in air, a secondary photoreaction can readily occur: oxidation of free ligand to phosphine oxide[19] or phosphate–phosphonate mixtures,[20] respectively. Since the latter classes of P(V) compounds are less likely to strongly coordinate than their unoxidized P(III) counterparts,[21] irradiation can conceivably generate high concentrations of coordinatively unsaturated centers in two ways: ligand dissociation *and* free ligand modification to prevent back-reaction (Scheme I). Previous qualitative observations have in fact indicated that oxygen is a cocatalyst for thermal processes built

(1) For an overview, see: *Adv. Organomet. Chem.* **1979**, *17*, 1, 105, 255, 319, 407, 449, and references therein.
(2) Wrighton, M. S.; Ginley, D. S.; Schroeder, M. A.; Morse, D. L. *Pure Appl. Chem.* **1975**, *41*, 671.
(3) Geoffroy, G. L.; Wrighton, M. S. "Organometallic Photochemistry"; Academic Press: New York, 1979.
(4) Koerner von Gustorf, E.; Grevels, F.-W. *Fortschr. Chem. Forsch.* **1969**, *13*, 366.
(5) Jennings, W.; Hill, B. *J. Am. Chem. Soc.* **1970**, *92*, 3199.
(6) Wrighton, M.; Hammond, G. S.; Gray, H. B. *J. Am. Chem. Soc.* **1970**, *92*, 6068.
(7) Nasielski, J.; Kirsch, P.; Wilputte-Steinert, L. *J. Organomet. Chem.* **1971**, *27*, C13.
(8) Wrighton, M.; Schroeder, M. A. *J. Am. Chem. Soc.* **1973**, *95*, 5764.
(9) Wrighton, M.; Hammond, G. S.; Gray, H. B. *J. Organomet. Chem.* **1974**, *70*, 283.
(10) Platbrood, G.; Wilputte-Steinert, L. *J. Organomet. Chem.* **1974**, *70*, 407.
(11) Wrighton, M. S.; Schroeder, M. A. *J. Am. Chem. Soc.* **1974**, *96*, 6235.
(12) Schroeder, M. A.; Wrighton, M. S. *J. Am. Chem. Soc.* **1976**, *98*, 551.
(13) Schroeder, M. A.; Wrighton, M. S. *J. Organomet. Chem.* **1977**, *128*, 345.
(14) Austin, R. G.; Paonessa, R. S.; Giordano, P. J.; Wrighton, M. S. *Adv. Chem. Ser.* **1978**, *No. 168*, 189.
(15) Sanner, R. D.; Austin, R. G.; Wrighton, M. S.; Honnick, W. D.; Pittman, C. V., Jr. *Inorg. Chem.* **1979**, *18*, 928.
(16) Wrighton, M. *Inorg. Chem.* **1974**, *13*, 905.
(17) Wrighton, M. S.; Abrahamson, H. B.; Morse, D. L. *J. Am. Chem. Soc.* **1976**, *98*, 4105.
(18) Choi, H. W.; Gavin, R. M.; Muetterties, E. L. *J. Chem. Soc., Chem. Commun.* **1979**, 1085.
(19) Geoffroy, G. L.; Denton, D. A.; Eigenbrot, C. W., Jr. *Inorg. Chem.* **1976**, *15*, 2310.
(20) Plumb, J. B.; Griffin, C. E. *J. Org. Chem.* **1963**, *28*, 2908.
(21) Darensbourg, D. J.; Walker, N.; Darensbourg, M. Y. *J. Am. Chem. Soc.* **1980**, *102*, 1213.

0020-1669/81/1320-1357$01.25/0